

**Determination of neutrino incoming direction
in the CHOOZ experiment and its application to
Supernova explosion location by scintillator detectors**

M. Apollonio^c, A. Baldini^b, C. Bemporad^b, E. Caffau^c, F. Cei^b, Y. Déclais^{e,1},
H. de Kerret^f, B. Dieterleⁱ, A. Etenko^d, L. Foresti^b, J. Georgeⁱ, G. Giannini^c,
M. Grassi^b, Y. Kozlov^d, W. Kropp^g, D. Kryn^f, M. Laiman^e, C.E. Lane^a,
B. Lefèvre^f, I. Machulin^d, A. Martemyanov^d, V. Martemyanov^d, L. Mikaelyan^d,
D. Nicolò^b, M. Obolensky^f, R. Pazzi^b, G. Pieri^b, L. Price^g, S. Riley^{g,h}, R. Reeder^h,
A. Sabelnikov^d, G. Santin^c, M. Skorokhvatov^d, H. Sobel^g, J. Steele^a, R. Steinberg^a,
S. Sukhotin^d, S. Tomshaw^a, D. Veron^f, and V. Vyrodov^f

^a*Drexel University*

^b*INFN and University of Pisa*

^c*INFN and University of Trieste*

^d*Kurchatov Institute*

^e*LAPP-IN2P3-CNRS Annecy*

^f*PCC-IN2P3-CNRS Collège de France*

^g*University of California, Irvine*

^h*University of New Mexico, Albuquerque*

¹*Now at IPN-IN2P3-CNRS, Lyon*

Abstract

The CHOOZ experiment ¹ has measured the antineutrino flux at about 1 Km from two nuclear reactors to search for possible $\bar{\nu}_e \rightarrow \bar{\nu}_x$ oscillations with mass-squared differences as low as 10^{-3} eV^2 for full mixing. We show that the analysis of the ~ 2700 $\bar{\nu}_e$ -events, collected by our liquid scintillation detector, locates the antineutrino source within a cone of half-aperture $\approx 18^\circ$ at the 68% C.L. . We discuss the implications of this result for locating a supernova explosion.

1 Introduction

Locating a ν -source in the sky is of primary importance in the case of galactic supernova (SN) explosions; particularly if the SN is not optically visible, either because it is hidden behind the dust of the galactic disk, or because the light emission follows the neutrino burst by hours or days. In this latter case, an early SN detection and location by neutrinos could allow observation of the evolution of the first optical stages.

Several pointing methods have been extensively discussed and compared in the literature [1],[2]:

- the identification of $\nu_e + e$ scattering events (a minority of the total number of events in most detectors);

¹The CHOOZ experiment is named after the new nuclear power station operated by Électricité de France (EdF) near the village of Chooz in the Ardennes region of France.

- the pronounced anisotropy of the charged-current (CC) $\nu_e + d$ and $\bar{\nu}_e + d$ reactions;
- the slight positron anisotropy in the CC reaction $\bar{\nu}_e + p \rightarrow n + e^+$;
- the triangulation between at least three detectors.

$\nu_e + e$ scattering events have an anisotropic angular distribution and, when observed in large detectors with good angular information, like the water Čerenkov detectors, permit localization of the SN. This technique was successfully applied to solar neutrinos by the KAMIOKANDE and the SUPERKAMIOKANDE (SK) experiments[6]. It has been shown[2] that this method can determine the direction of a Supernova, at a distance of 10 Kpc, within a $\sim 5^\circ$ cone (one-sigma angular width). The other methods mentioned above have less precise pointing capabilities.

We show in this paper that, in the case of large scintillation detectors, another tool, based on the inverse-beta-decay reaction

$$\bar{\nu}_e + p \rightarrow n + e^+, \quad (1)$$

is also capable of providing a good determination of Supernova direction. Although the positron is emitted almost isotropically in this reaction, the neutron has an energy-dependent maximum angle of emission and an associated Jacobian peak in its angular distribution. The neutron therefore retains a memory of the neutrino direction, which survives even after collisions with the protons of the moderating scintillator medium.

A first study along this line [7] was performed for the MACRO experiment and its SN detection capabilities, with results which were not encouraging. However, the single-vessel structure of the CHOOZ experiment and its superior energy and position resolutions appeared more promising. An average displacement of neutrons with respect to positrons has been observed in previous reactor neutrino experiments [3, 4]. In CHOOZ we were able to test this neutron recoil method and to use it for locating the reactor-neutrino source.

The CHOOZ experiment has also been a good test bench for our Montecarlo simulations of the slowing down and capture of neutrons in a scintillator, and for our methods of event reconstruction in a single-vessel structure observed by photomultipliers. We believe that extrapolation from CHOOZ to much larger volume scintillator detectors can be reliably made, and we therefore evaluate the SN locating capabilities of future scintillator detectors in the 1000 tons range, like BOREXINO and KAMLAND.

2 Antineutrino detection in scintillator experiments

$\bar{\nu}_e$'s are detected in scintillator experiments via inverse-beta-decay (Reaction 1). The $\bar{\nu}_e$ signature is a delayed coincidence between the prompt e^+ signal (boosted by the two 511 KeV annihilation gamma rays) and the signal from the neutron capture. The target material is a hydrogen-rich (free protons) paraffinic liquid scintillator; in CHOOZ the scintillator is loaded with gadolinium.

2.1 Positron displacement

The cross section for the $\bar{\nu}_e$ capture process [8, 2, 5] can be written for low energy antineutrinos as

$$\frac{d\sigma}{d\Omega} = \frac{G_f^2}{4\pi^2} p_{e^+} E_{e^+} \{ (1 + 3F_4^2) + (1 - F_4^2) \cos\theta_{e^+} \} \quad (2)$$

With the value of F_4 obtained from β -decay one derives the positron angular distribution in the laboratory

$$P(\theta_{e^+}) = \text{Constant} \times (1 - 0.102 \cos\theta_{e^+}) \quad (3)$$

This tiny anisotropy could in principle be employed if one had an extremely large number of events. But this is not normally the case for SN explosions nor was it for the CHOOZ long-baseline reactor-neutrino experiment. In the case of CHOOZ, by averaging Eqn. 3 over the solid angle and positron spectrum, one obtains an average positron displacement with respect to the interaction of ~ -0.05 cm which, as we will see later, is not measurable with our spatial resolution and statistics. In [2, 5] the dependence of the $\cos\theta_{e^+}$ coefficient on the positron energy is discussed. Such a dependence does not affect the conclusions of this paper because the average positron displacement remains negligibly small.

2.2 Neutron displacement

Figure 1 (right) shows the scatter plot θ_n (angle with respect to the incident neutrino direction) versus T_n (kinetic energy) for neutrons emitted in Reaction 1 with our detected reactor-neutrino spectrum (left). The neutron kinetic energy extends up to ~ 100 KeV and the angle with respect to the incoming neutrino direction is limited to values below $\sim 55^\circ$. The separated curves visible in the lower-left part of the picture are caused by the $\bar{\nu}_e$ energy binning and by the logarithmic scale adopted for the x-axis. They show how the $\theta_n - T_n$ dependence changes as a function of the $\bar{\nu}_e$ energy.

The neutron slowing-down phase[10], in which its energy is reduced to the thermal equilibrium value, is a non-isotropic process which preserves a memory of the initial neutron direction. In each elastic scattering the average cosine of the outgoing neutron with respect to the incoming direction is:

$$\overline{\cos\theta_n} = \frac{2}{3A} \quad (4)$$

where A is the atomic number of the scattering nucleus. The direction is therefore best preserved by scatterings on hydrogen, which in fact is the most probable occurrence since the elastic scattering cross section on hydrogen is larger than that on carbon for energies below 1 MeV.

Slowing-down is an extremely efficient process in which the neutron energy rapidly decreases (an average factor of two for each scattering on hydrogen). Since

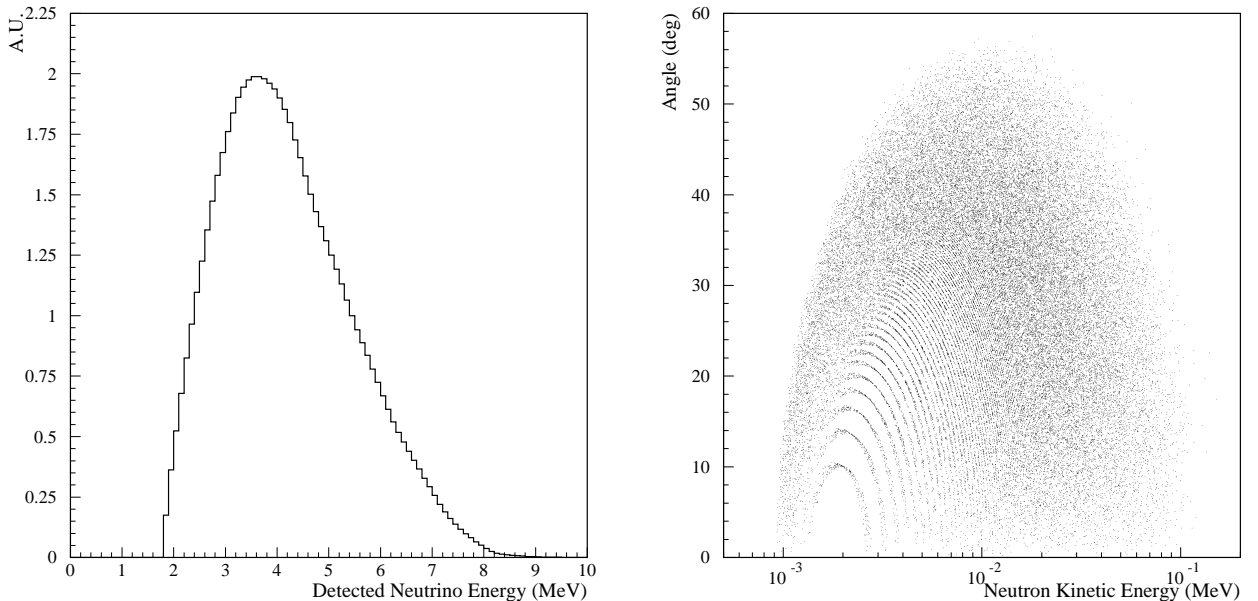


Figure 1: Detected reactor neutrino energy spectrum (left) and neutron angle with respect to the incident neutrino direction versus its kinetic energy(right).

the scattering cross section is a decreasing function of the neutron energy, it follows that the neutron mean free path (λ_s) rapidly diminishes during moderation. As a matter of fact the distance from the production point travelled by neutrons before being thermalized is determined by the first two or three scatterings, in which a memory of the initial direction is preserved, according to Eqn. 4.

The subsequent (isotropic) diffusion process does not alter the average neutron displacement along the neutrino direction. In CHOOZ this average displacement is ~ 1.7 cm.

In Table 1 we give some of the parameters characterizing the moderation and diffusion phases (\hat{n}_s : average number of scatterings; t_d : time duration; $\sqrt{r^2}$: average square distance, which does not include the neutron angular distribution of Reaction 1) computed for neutrons from reactor-neutrino interactions in the CHOOZ liquid scintillator.

Table 1: Parameters characterizing the neutron moderation and diffusion phases in CHOOZ (see text)

	\hat{n}_s	t_d	$\sqrt{r^2}$
Moderation	10 – 14	$9 \mu s$	≈ 6 cm
Diffusion	≈ 20	$\sim 30 \mu s$	≈ 3 cm

3 Description of the CHOOZ Experiment

A description of the CHOOZ experiment, its analysis methods, and its initial results has been previously published [9]. Here we recall only the points needed for the present discussion.

3.1 The neutrino source

The Chooz power station has two pressurized-water reactors with a total thermal power of $8.5 \text{ GW}_{\text{th}}$. The average direction of the two reactors in the CHOOZ polar coordinate system was measured by standard surveying techniques to be $\phi = (-50.3 \pm 0.5)^\circ$ and $\theta = (91.5 \pm 0.5)^\circ$, where θ is the zenith angle and the origin of the azimuthal (ϕ) coordinate is arbitrarily fixed.

3.2 The Detector

The Gd-loaded scintillator target is contained in an acrylic vessel of precisely known volume immersed in a low-energy calorimeter made of unloaded liquid scintillator. Gd was chosen because of its large neutron-capture cross section and large neutron-capture γ -ray energy release ($\sim 8 \text{ MeV}$, well separated from the natural radioactivity background).

The detector is made of three concentric regions:

- a central 5-ton target in a transparent acrylic container filled with a 0.09% Gd-loaded scintillator (“region 1”);
- an intermediate 17-ton region (70 cm thick) equipped with 192 eight-inch PMT’s (15% surface coverage, ~ 130 photoelectrons/MeV) used to protect the target from PMT radioactivity and to contain the gamma rays from neutron capture (“region 2”);
- an outer 90-ton optically-separated active cosmic-ray muon veto shield (80 cm thick) equipped with two rings of 24 eight-inch PMT’s (“region 3”).

The detector is simple and easily calibrated, and its behaviour can be well checked. Six laser flashers are installed in the three regions together with calibration pipes to allow the introduction of radioactive sources.

Particularly important for this paper are the neutron calibrations performed by using ^{252}Cf , a spontaneous fission source emitting several prompt, energetic neutrons ($\overline{E} \sim 2 \text{ MeV}$) and γ rays with energies up to $\sim 10 \text{ MeV}$.

The detector can be reliably simulated by the Montecarlo method .

4 Data analysis

4.1 Event reconstruction

The determination of the direction to the reactors relies on the energy and position reconstruction of individual events.

The method presented here is based on the data obtained from the VME ADC's (192 PMT's divided into 24 groups ("patches") of 8 PMT's each) viewing regions 1 and 2. We checked that this grouping does not significantly affect the energy and position determination. Using the additional information provided by the TDC's might improve the position resolution.

Each event is reconstructed by minimizing the Poissonian χ^2

$$\chi^2 = 2 \times \sum_{i=1}^{24} [(N_{th}^i - N_{obs}^i) + N_{obs}^i \times \log(\frac{N_{obs}^i}{N_{th}^i})] \quad (5)$$

where N_{obs}^i and N_{th}^i are the measured and expected numbers of photoelectrons of the i_{th} patch, for a given event's energy and position.

A Poissonian χ^2 is used due to the frequent occurrence of low numbers of photoelectrons in some PMT patches; this demands the application of the correct statistics.

The conversion factors from the measured ADC charges to the numbers of photoelectrons are obtained for each patch from the single-photoelectron peak position measured by flashing the central laser at very low intensity.

The patch electronic gains have differences caused by the behaviour of the active electronic components (fan-in, fan-out etc.) present after the PMT's. The patch's relative gains are measured frequently using the 8 MeV absorption peak of the neutrons emitted by a ^{252}Cf source placed at the center of the detector. Corrections are applied for the different solid angles of the various patches.

The predicted number of photoelectrons for each patch is computed by considering a local deposit of energy, resulting in a number of visible photons that are tracked to the PMT's taking into account the different attenuation lengths of region 1 and 2 scintillators.

To reduce computing time PMT's are considered to be flat and Rayleigh scattering is neglected. Despite these simplifications the time needed for reconstructing one event is of the order of one second on a Pentium processor.

4.2 Montecarlo simulation

The detector response was simulated by means of the CERN GEANT package. The complete geometry was taken into account. Particular attention was devoted to low-energy neutrons ($E_n < 10$ MeV) by using specially designed routines which modeled the elastic scattering and capture on individual elements of the scintillators and acrylic vessel, employing the relevant experimental cross sections [11]. Neutron capture on Gadolinium was simulated for the two main isotopes: ^{155}Gd and ^{157}Gd . Following a capture on Gd either two monoenergetic photons or a varying number of photons, obtained by considering transitions to intermediate energy levels with a probability proportional to the cube of the energy difference, were emitted [12].

Collection of the light generated by local energy deposits was performed under the same approximations described in section 4.1.

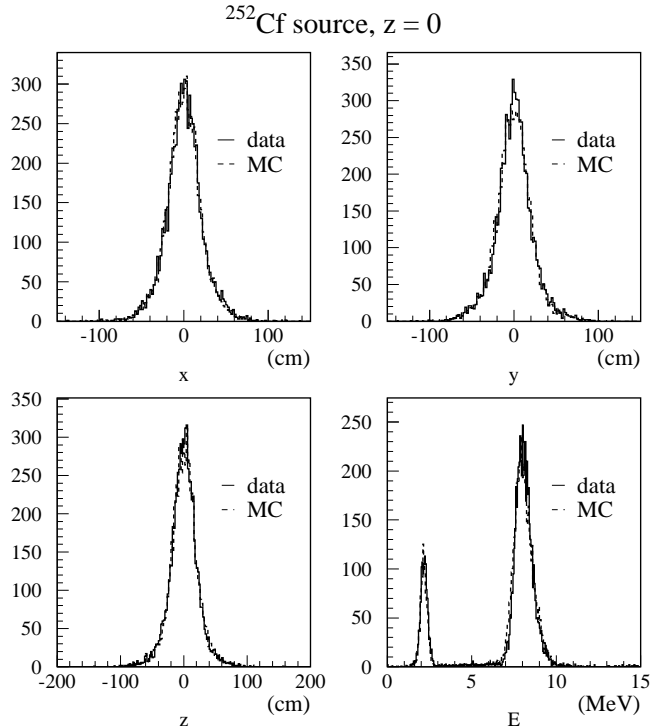


Figure 2: Reconstructed position and energy for neutrons emitted by a californium source at the center of the apparatus.

In Figure 2 we show the reconstructed position and energy for neutrons emitted by a ^{252}Cf source at the apparatus center (continuous line). The agreement with the superimposed Montecarlo simulation (dashed line) is very good.

4.3 Candidate selection and comparison with the Monte-carlo simulation

The candidate selection is based on the following requirements:

- energy cuts on the neutron candidate (6 – 12 MeV) and on the e^+ (from hardware threshold energy $E_{thr} \sim 1.3$ MeV to 8 MeV),
- a time cut on the delay between the e^+ and the neutron (2 – 100 μs),
- spatial cuts on the e^+ and the neutron (distance from the PMT wall > 30 cm and distance between the n and e^+ vertices < 100 cm).

The total number of candidates for the complete data taking period with reactors on is ~ 2700 . We also collected ~ 200 background events during two reactor-off periods: in the middle (October 1997) and right after the end (February 1998) of the reactor-on data taking period.

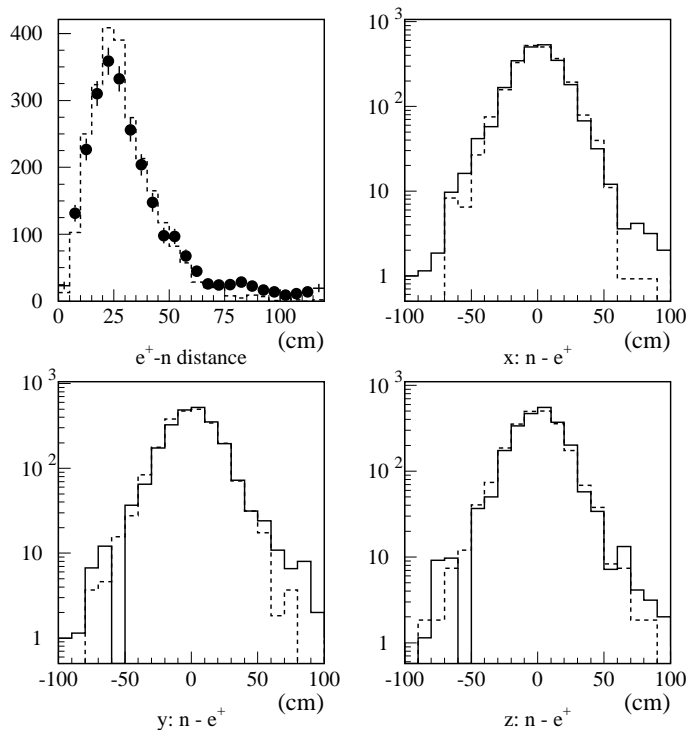


Figure 3: Background-subtracted distributions of the difference between the coordinates of neutrons and positrons, and the positron-neutron distance for the candidates (continuous lines) and the expected Montecarlo distributions (dashed lines).

Figure 3 shows the background-subtracted distributions of the difference between the coordinates of neutrons and positrons for the candidates (continuous lines). Also shown is the positron-neutron distance distribution. The expected Montecarlo distributions (dashed lines) are superimposed on the experimental data. The discrepancies are attributed to the simplified light collection scheme adopted in the Montecarlo. We also point out that, by utilizing the difference between the neutron and positron positions, most systematic errors in the absolute reconstructed coordinates are canceled out.

For this analysis we required the combined thermal power of both reactors to be greater than 3 GW in order to increase the signal to background ratio. The candidates reduce to ~ 2500 after this condition is applied.

5 Location of the reactors by neutrino events

5.1 The technique used

As seen in section 2, while the average positron displacement with respect to the neutrino interaction point is not measurable, a sizable average displacement of the

neutron capture point along the neutrino incoming direction is predicted. In order to measure the direction of this average displacement we define for each neutrino candidate the unit vector \hat{X}_{pn} having its origin at the positron reconstructed position and pointing to the neutron capture location.

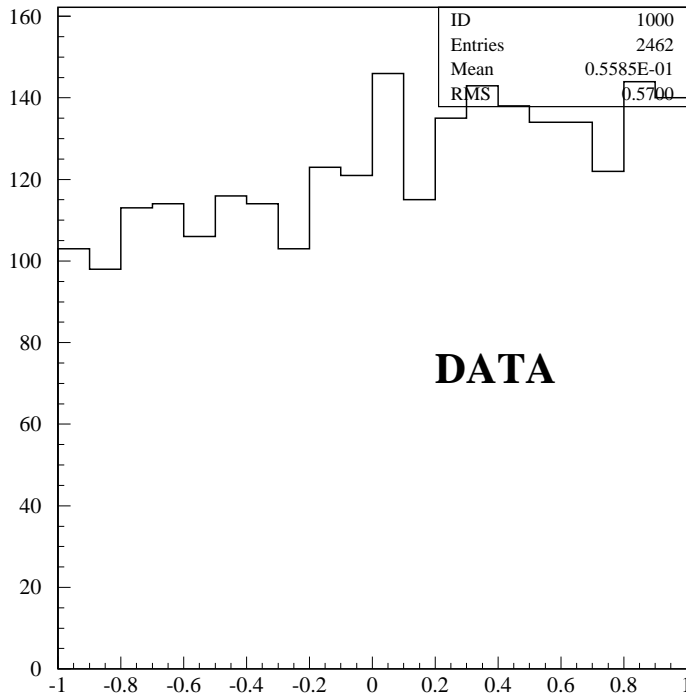


Figure 4: Distribution of the projection of the positron-neutron unit vector along the known neutrino direction.

The distribution of the projection of this vector along the known neutrino direction is shown for candidates in figure 4. This distribution can be compared with Fig. 5 which shows the distribution expected from a Montecarlo simulation with higher statistics ($\sim 5,000$ events).

Both distributions are forward peaked although their R.M.S. values (0.570 and 0.565, respectively) are not far from that of a flat distribution ($\sigma_{flat} = 1/\sqrt{3} \simeq 0.577$).

We define \vec{p} as the average of vectors \hat{X}_{pn}

$$\vec{p} = \frac{1}{N} \sum_i \hat{X}_{pn} \quad (6)$$

The measured neutrino direction is the direction of \vec{p} .

In order to evaluate the uncertainty in this value we need to know the expected distribution of \vec{p} . Let us assume the neutrino direction lies along the z axis. \vec{p} is the sum (divided by N) of N variables of which we know the average (\vec{p} itself

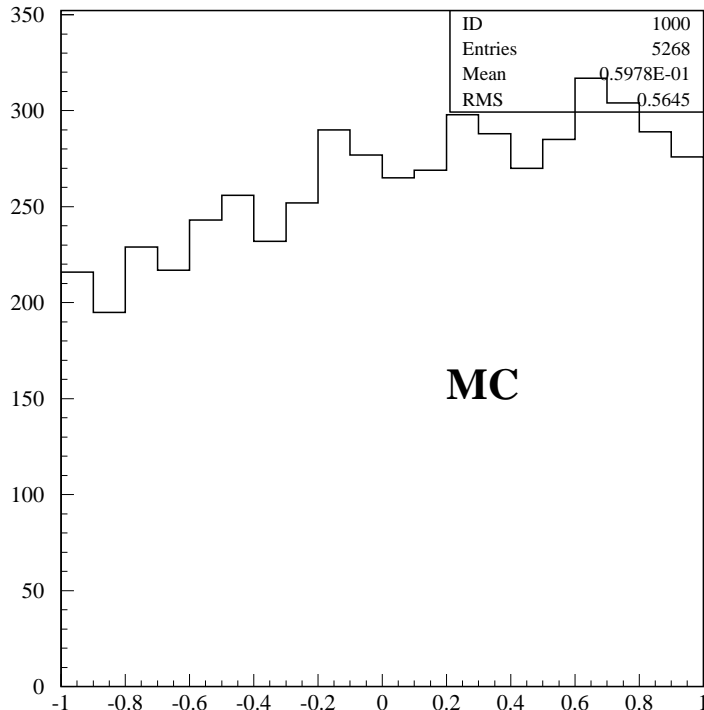


Figure 5: Distribution of the projection of the Montecarlo positron-neutron unit vector along the known neutrino direction.

$= (0, 0, |\vec{p}|)$ and σ (we can safely assume $\sigma = 1/\sqrt{3}$ for the three components, as seen above). From the central limit theorem it follows therefore that the distributions of the three \vec{p} components are gaussians with $\sigma = 1/\sqrt{3N}$ centered at $= (0, 0, |\vec{p}|)$. An uncertainty on the measurement of the neutrino direction can therefore be given as the cone around \vec{p} which contains 68% of the integral of this distribution.

Another direction estimator we tried to use is the simple average of the differences between the neutron and positron reconstructed positions:

$$\vec{q} = \frac{1}{N} \sum_i (\vec{X}_n - \vec{X}_p) \quad (7)$$

The results obtained using this estimator are very close to those one gets with the first one, although the corresponding uncertainties are always a bit ($\sim 10\%$) larger (this is also true when the methods are applied to Montecarlo generated events). In the following we will therefore quote only the results obtained with the \vec{p} estimator.

5.2 Experimental result

Table 2 shows our result for the measured direction, compared with the Montecarlo predictions for a sample with the same statistics. The measured direction is in

agreement (with a 16% probability) with that expected while it has a negligible probability of being a fluctuation of an isotropic distribution.

The measured average positron–neutron displacement for candidates turns out to be $1.9 \pm 0.4\text{cm}$, in agreement with the predicted value.

Table 2: Measurement of neutrino direction: data and Montecarlo

	$ \vec{p} $	ϕ	θ	Uncertainty
Data	0.055	-70°	103°	18°
MC	0.052	-56°	100°	19°

We checked that the same technique, when applied to ^{252}Cf runs in which prompt γ 's (selected by requiring the first event recorded to have an energy in the range of 3 to 7 MeV) are used to fake positrons, give results compatible with isotropic distributions.

6 Locating Supernovæ

We applied the above technique to the determination of the neutrino direction from a Supernova in a liquid scintillator experiment. The difference in the neutrino energy spectrum (the average detected neutrino energy for a Supernova is $\sim 17\text{MeV}$ [13] to be compared to the 4 MeV of the reactor case) has two major consequences:

- the maximum neutron angle with respect to the neutrino direction increases (in figure 6 we show the equivalent of Fig. 1 for a Supernova neutrino energy distribution)
- the higher neutron energy implies lower cross–sections which in turn imply higher displacements of the average capture point from that of production.

Clearly these effects have opposite influences (the first, negative; the second, positive) on the neutrino direction determination. The combination of the two effects was evaluated by using the full CHOOZ Montecarlo simulation.

We used the following Supernova $\bar{\nu}_e$ energy distribution [13]:

$$\frac{dN}{dE} = C \frac{E^2}{1 + e^{\frac{E}{T}}} \quad (8)$$

with $T = 3.3\text{MeV}^2$ and considered the Supernova to be at 10 Kpc.

We generated 5000 neutrino interactions in an experiment with the same geometry, the same position resolution and the same target (Gd-loaded liquid scintillator)

²Other authors[2] use more energetic spectra which (as we will see shortly) improve the possibility of determininig the $\bar{\nu}_e$ direction with the present method.

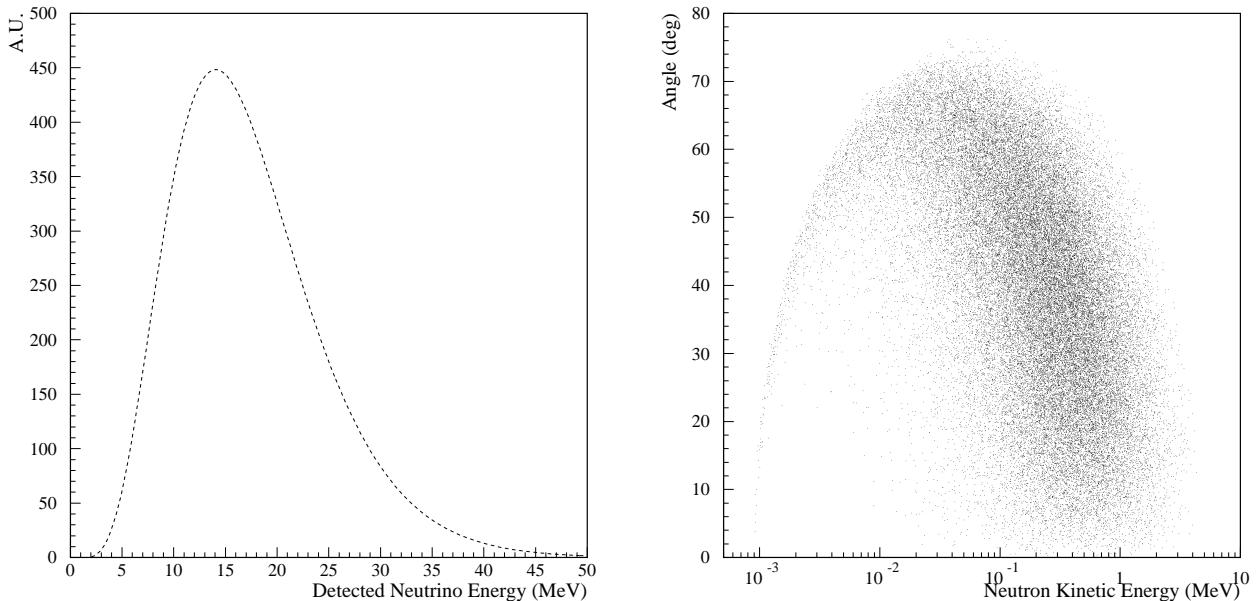


Figure 6: Detected Supernova neutrino energy spectrum (left) and neutron angle with respect to the incident neutrino direction versus its kinetic energy(right).

as the CHOOZ experiment. This number of events, for a Supernova at 10 Kpc, could be detected in a liquid scintillator experiment with mass equal to that of SK. Such an experiment is not even foreseen at present, but our aim here is just to compare the possibilities of the technique we are investigating with those offered by the neutrino elastic scattering in SK. We chose the neutrino direction to have a zenith angle of zero degrees (which implies an undefined azimuthal angle).

The results of applying the technique described in paragraph 5.1 to this case are shown in table 3 (first line). The resulting uncertainty in the direction measurement is 8.8° .

Table 3: Measurement of the Supernova neutrino direction: Montecarlo events. The results in the second line are obtained by requiring the positron–neutron distance to be larger than 20 cm. Note that the ϕ angle determination is irrelevant since neutrinos are directed along the zenith axis.

$ \vec{p} $	ϕ	θ	Uncertainty
0.079	111°	11°	8.8°
0.102	66°	8°	8.4°

From this result it follows that the increase in the neutron production–capture distance dominates over the broadening of the possible neutron emission angles. The

average positron–neutron displacement in this case turns out to be ~ 2.5 cm.

We also investigated the effects on the direction determination of possible event-by-event cuts on the positron energy or on the positron–neutron distance. The only statistically significant (though small) improvement was obtained by requiring the positron–neutron distance to be larger than 20 cm, which corresponds to a reduction of the neutrino sample from ~ 5000 to ~ 3400 events. The results obtained applying this cut are also shown in table 3.

We finally point out that in the Supernova case the background for Reaction 1 is negligible since the duration of the neutrino burst is of the order of 10 seconds.

7 Conclusions

The CHOOZ experiment demonstrates for the first time the use of Reaction 1 for measuring the average neutrino direction.

This technique could be important in Supernovæ neutrino detection with liquid scintillator-based experiments, which have the advantage of possessing a superior energy resolution compared to Čerenkov detectors.

By using the full CHOOZ Montecarlo simulation we showed that in an experiment with a sufficiently high mass and adequate position resolution, it is possible to measure the sky coordinates of a Supernova at 10 Kpc with an uncertainty larger by only a factor two ($\sim 9^\circ$ compared to 5°) than that attainable by using the angular distribution of neutrino elastic scattering in SK.

These results represent also an important check of the event reconstruction procedure of the CHOOZ experiment and enhances our confidence in the analysis methods employed.

Acknowledgements

Construction of the laboratory was funded by Électricité de France (EdF). Other work was supported in part by IN2P3–CNRS (France), INFN (Italy), the United States Department of Energy, and by RFBR (Russia). We are very grateful to the Conseil Général des Ardennes for having provided us with the headquarters building for the experiment. At various stages during construction and running of the experiment, we benefited from the efficient work of personnel from SENA (Société Electronucléaire des Ardennes) and from the EdF Chooz B nuclear plant. Special thanks to the technical staff of our laboratories for their excellent work in designing and building the detector.

References

- [1] A. Burrows *et al.*, Phys. Rev. D**45** (1992) 3361.
- [2] J.F. Beacom and P. Vogel, astro-ph/9811350 (1998).

- [3] G. Zacek *et al.*, Phys. Rev. D**34** (1986) 2621.
- [4] B. Achkar *et al.*, Nucl. Phys. B**434** (1995) 503.
- [5] J.F. Beacom and P. Vogel, astro-ph/9903554 (1999).
- [6] For a review see M.Koshihara, proceedings of the “*XVIIIth International Conference on Neutrino Physics and Astrophysics*”, Takayama, June 1998.
- [7] C. Bemporad for the MACRO collaboration, proceedings of the “*Third International Workshop on Neutrino Telescopes*”, Venice (1991).
C.Bemporad for the CHOOZ collaboration, proceedings of the “*XVIIIth International Conference on Neutrino Physics and Astrophysics*”, Takayama, June 1998.
- [8] T.K. Gaisser *et al.*, Phys. Rev. D**34** (1986) 822.
- [9] M. Apollonio *et al.*, Phys. Lett. B**338** (1998) 383.
- [10] For a simple description of the moderation and diffusion processes see E. Persico, *Lezioni sulla fisica del reattore*, Comitato Nazionale per le Ricerche Nucleari, Roma (1960).
For a more complete work see E. Amaldi, “*The production and Slowing Down of Neutrons*” in S. Fluegge, *Encyclopedia of Physics*, Springer-Verlag, vol. 38.2 (1959).
- [11] McLane, Dunford, Rose, “*Neutron Cross Sections*” Brookhaven N.L. Academic press Inc. vol. 1A, 1B.
- [12] H. De Kerret and B. Lefèvre, L.P.C. 88 01, Collège de France (1988).
- [13] S.A. Bludman and P.J. Schinder, *Astrophys. J.* **326** (1988) 288.